

AD-A039 194

CALSPAN CORP BUFFALO N Y

F/G 20/5

TWO DIMENSIONAL EFFECTS IN LASER SOLID SIMULATION STUDIES.(U)

OCT 76 J W DAIBER, H M THOMPSON

F44620-74-C-0004

UNCLASSIFIED

CALSPAN-WG-5376-A-3

AFOSR-TR-77-0606

NL

1 OF 1
ADA039194



AFOSR - TR - 77 - 0606

12
b.s.

ADA 039194

alspan

Technical Report



AD No. _____
DDC FILE COPY

DDC
RECEIVED
MAY 10 1977
R
D

DISTRIBUTION STATEMENT A

Approved for public release;
Distribution Unlimited

Corporation
Buffalo, New York 14221

AIR FORCE OFFICE OF SCIENTIFIC RESEARCH (AFSC)
NOTICE OF TRANSMITTAL TO DDC
This technical report has been reviewed and is
approved for public release IAW AFR 190-12 (7b).
Distribution is unlimited.
A. D. BLOSE
Technical Information Officer

ACCESSION for

OTIS	White Section	<input checked="" type="checkbox"/>
DO9	Buff Section	<input type="checkbox"/>
UNANNOUNCED		<input type="checkbox"/>
JUSTIFICATION		

SECTION/AVAILABILITY CODES

REG. and/or SPECIAL

A

J.W. Daiber and H.M. Thompson

Prepared For:

OCTOBER 1976
CONTRACT NO. F44620-74-C-0004
FINAL TECHNICAL REPORT

PREPARED FOR:

J. W. Daiber

APPROVED BY:

C.E. Treanor, Head
Aerodynamic Research Department

H.M. Thompson
H.M. Thompson

See 1473

DDC
RECEIVED
MAY 10 1977
RECEIVED

DISTRIBUTION STATEMENT A

Approved for public release;
Distribution Unlimited

FOREWORD

This final report on Contract F44620-74-C-0004 was prepared by the Aerodynamic Research Department of Calspan Corporation, Buffalo, New York 14221 for the Physics Division of the Air Force Office of Scientific Research (AFSC) USAF. This work was a continuation of that performed by Calspan for AFOSR on Contract F44620-71-C-0102. The research reported herein was accomplished under the technical cognizance of Dr. T. C. Collins, Capt. A. A. Abela, and Lt. Col. A. R. Cole.

TABLE OF CONTENTS

<u>Section</u>		<u>Page</u>
	FOREWORD	ii
I	INTRODUCTION	1
II	TWO-DIMENSIONAL GROWTH OF A BLEACHING WAVE	7
III	TWO-DIMENSIONAL GROWTH OF LASER-DRIVEN WAVES IN A HYDROGEN FREE JET	10
IV	ELECTRON-TEMPERATURE AND SPONTANEOUS MAGNETIC FIELD MEASUREMENTS IN A LASER-IRRADIATED FREE JET.	16

Section I

INTRODUCTION

The study of laser irradiation of materials is of interest because of applications to target damage¹ and pellet fusion.² For high peak-power lasers where fluid pressures of 500 to 1000 kbars are generated, the interaction process can be modeled by neglecting the strength of the material.³ At late times, after the laser pulse has terminated, the strength of the laser-driven compression waves decrease. The strength of the target material then becomes increasingly important in determining the propagation of the stress waves and the resulting material damage.⁴ For the creation of fusion in hydrogen pellets, the laser-driven compression waves undergo a continuous acceleration while they implode⁵ and the strength of the material is not of interest for practical cases. In analyzing this early-time motion, it is proper to treat the material as though it were an inviscid fluid, and to replace its constitutive relation by a thermodynamic equation of state.³

The objective of the current program was to study the early-time motion in sufficient detail that the wave system existing at the time of decay into an elastic stress wave could be predicted. Thus more accurate target-damage estimates would then be possible since the peak stresses in a material

-
1. R. R. Rudder, Momentum Transfer to Solid Target Discs by Pulsed One-Micron Radiation, Laser Digest, Air Force Weapons Lab. AFWL-TR-73-273, p. 137 (December 1973).
 2. K. A. Brueckner and S. Jorna, Laser-Driven Fusion, Rev. Mod. Phys. 46, 325 (1974).
 3. R. S. Cooper, Motion of Solid D₂ Under Laser Irradiation. AIAA J. 11, 831 (1973).
 4. W. J. Rae, "Analytical Studies of Impact-Generated Shock Propagation" Survey and New Results", Chapter 6, High-Velocity Impact Phenomena, ed. by R. Kinslow Academic Press (1970).
 5. J. W. Daiber, A. Hertzberg and C. E. Wittliff, Laser-Generated Implosions. Phys. of Fluids 9, 617 (1966).

are closely coupled to the initial stress distribution. For the present studies, the opaque target has been replaced by a gaseous free-jet.⁶ This gaseous target simulates the solid during the early time when the hydro-equations are adequate for describing the wave motion in the solid. The gaseous target offers the advantages of simplified diagnostics and higher energy loadings per target particle.

The work performed in this program can be divided into three parts; analytical studies of fluid motion, measurement of two-dimensional plasma growth, and measurement of spontaneous magnetic fields. A summary of the work performed in the first two areas has been published in the scientific literature. Reprints of these articles constitute the following two sections of this report. A technical paper describing the spontaneous magnetic field measurements has been submitted for publication. Section IV of this report contains a preprint of the submitted paper.

In addition to the publication of the work performed on this contract, several oral presentations of the program findings were made at technical meetings. These were:

"Spontaneously Generated Magnetic Fields from a Laser Irradiated Free Jet", Plasma Physics Meeting of the American Physical Society, 10-14 November 1975 in Tampa, Florida.

"Electron Temperature and Plasma Growth Measurements in Laser Irradiated Free Jets", Plasma Physics Meeting of the American Physical Society, 28-31 October 1974 in Albuquerque, New Mexico.

"Two-Dimensional Shock-Wave Growth in Laser Irradiated Hydrogen Jets", Plasma Physics Meeting of the American Physical Society, 31 October - 3 November 1973 in Philadelphia, Pennsylvania.

Copies of the abstracts of these papers are contained on the following three pages.

6. H. M. Thompson, R. G. Rehm, and J. W. Daiber, Laser Driven Waves in a Freely Expanded Gas Jet, J. Appl. Phys. 42, 310 (1971).

Abstract Submitted
for the Plasma Physics Divisional Meeting of the
American Physical Society
10-14 November 1975

Physics and Astronomy
Classification Scheme
Number

Bulletin Subject Heading
in which Paper should be placed

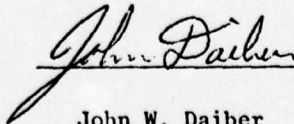
Laser-Matter Interaction

Spontaneously Generated Magnetic Fields from a
Laser Irradiated Free Jet. H. M. THOMPSON and J.W.DAIBER,
Calspan Corp.--The objective of this program is to study
spontaneously generated magnetic fields produced in a
target by high-power laser radiation. For these studies
the target is an axisymmetric, supersonic free jet which
is irradiated on axis. The transparency of the target
permits measurement of the velocity of the forward-facing
waves that propagate into the high pressure plenum. Small
high-frequency inductive probes are used to observe the
azimuthal fields. Measurements of the radial and axial
distribution are obtained at six positions surrounding
the plasma. In addition, soft x-ray detectors have been
used to measure the plasma electron temperature. Simul-
taneous measurements of the magnetic field distribution,
plasma dynamics and electron temperature have been ob-
tained in hydrogen and nitrogen at plenum pressures up to
10 atm. Magnetic field strengths comparable to those ob-
served from solid targets have been recorded. The vol-
umetric growth of the plasma is restricted to a region
which is notably less than the cone of the incident
laser field.

*Submitted by J. W. DAIBER

+Sponsored by AFOSR/AFSC

Submitted by



John W. Daiber

Calspan Corporation
P. O. Box 235
Buffalo, New York 14221

Abstract Submitted
for the Plasma Physics Meeting of the
American Physical Society
28-31 October 1974

Physical Review
Analytic Subject Index
Number

Bulletin Subject Heading in
which Paper should be placed

Plasma Physics
Number 92

Electron Temperature and Plasma Growth Measure-
ments in Laser Irradiated Gas Jets.* H. M. THOMPSON,
R. G. REHM, and J. W. DAIBER, Calspan Corporation,
Buffalo, N.Y.--X-ray flux measurements have been made on
plasma produced in a freely expanding nitrogen gas jet.
An electron temperature has been inferred from the x-ray
measurements using a metal-foil absorption spectrometer.
Nitrogen gas has been expanded supersonically through an
orifice into an evacuated chamber to produce a large axial
density gradient. The laser, axially aligned with the
jet, is focused into the jet near the orifice. Irradia-
tion produces breakdown and creates a luminous plasma
which expands both into the evacuated region and inward
toward the higher density region. Reservoir density and
laser intensity have been varied. As in earlier studies
the average growth velocity has been found to correlate
with laser intensity divided by reservoir density. Cor-
relations between the electron-temperature, the growth
velocity and the parameter laser power divided by reser-
voir pressure are discussed.

*Submitted by R. G. Rehm.

+Sponsored by the Air Force Office of Scientific
Research (AFSC).

Submitted by

Ronald Rehm

R. G. REHM

Calspan Corporation

P. O. Box 235

Buffalo, New York 14221

Abstract Submitted
for the Plasma Physics Meeting of the
American Physical Society
31 October - 3 November 1973

Physical Review
Analytic Subject Index
Number _____

Bulletin Subject Heading
in which Paper should be placed

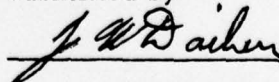
Plasma Physics
Number 9C - Laser Produced Plasmas: General

5C8 Two-Dimensional Shock-Wave Growth in Laser
Irradiated Hydrogen Jets*⁺ H. M. THOMPSON,
R. G. REHM, and J. W. DAIBER, Calspan Corporation,
Buffalo, N. Y. 14221--Hydrogen gas has been expanded
supersonically into an evacuated chamber to produce a
large axial density gradient. The laser, aligned with the
jet, has its output focused into the jet near the orifice.
Irradiation produces breakdown and creates a luminous
region which expands through the orifice into the high-
density reservoir. By variation of the reservoir density
and of laser intensity, the dynamical response can be
observed over a wide range of the governing parameters.
Photographs of the growth rate of the luminous region
and the subsequent shock wave in the axial and transverse
directions have been obtained on the same streak record.
The trajectory of the shock wave is a continuation of that
of a luminous front. The average growth velocity has been
found to correlate with the laser intensity divided by the
reservoir density to the one-third power. The character
of the two-dimensional shock wave has been predicted by
a theoretical model based on a self-similar solution which
is valid until later times.

*Submitted by J. W. Daiber

⁺Sponsored by the Air Force Office of Scientific Research
(AFSC).

Submitted by



J. W. Daiber

Calspan Corporation

P. O. Box 235

Buffalo, N. Y. 14221

The principal investigator for this program was Dr. John W. Daiber. However, for a portion of the period covered by this contract Dr. Ronald G. Rehm was co-principal investigator. All of the laboratory experiments were carried out by Mr. Herbert M. Thompson.

Section II Two-dimensional growth of a bleaching wave

Ronald G. Rehm

Calspan Corporation, Buffalo, New York 14221

(Received 3 December 1973; final manuscript received 15 February 1974)

An analytical solution is presented which describes the axisymmetric growth of a high-temperature region heated by laser radiation, known as a bleaching wave. Constant-temperature profiles for the wave are shown for ruby laser radiation and for CO₂ laser radiation incident upon a plasma.

Growth of a high-temperature region heated by laser radiation, known as a heating wave or a bleaching wave, has been predicted for some time in the literature.¹⁻³ A scheme for "long wavelength heating" of a magnetically confined plasma using a CO₂ laser^{4,5} has renewed interest in this phenomenon⁶⁻⁸ since it appears that experimental conditions have been achieved for observing it.⁶ The purpose of this note is to describe an analytical extension to the solution for the one-dimensional model of this phenomenon^{1,2} which allows the calculation of its two-dimensional (axisymmetric) growth. The two-dimensional features of the bleaching wave will be particularly useful for comparison with framing photographs of the phenomenon obtained in experiments.

Consider the laser heating of plasma at a plasma-vacuum interface as shown in Fig. 1. An analytical solution describing a bleaching wave can be obtained when the radiative energy is absorbed at a very rapid rate and the plasma does not have a chance to respond dynamically. Physically, this solution represents the two-dimensional, time-dependent heating of the plasma during the early part of the interaction. The high-intensity laser pulse is absorbed by the plasma and a wave of heating progresses into the plasma. This bleaching wave is characterized by a rapid increase in temperature in the material near the plasma-vacuum interface with the density remaining essentially constant and little motion being induced. Because of the form of the absorption coefficient, which is assumed to be that appropriate for inverse bremsstrahlung, the absorption by the plasma decreases rapidly as the temperature within the plasma increases. The heated plasma near the interface becomes more transparent or bleached to the laser radiation as time progresses, and the deeper layers of the plasma are exposed to and can absorb more of the incident radiation. In this way the heating progresses deeper into the plasma until the plasma has time to respond dynamically.

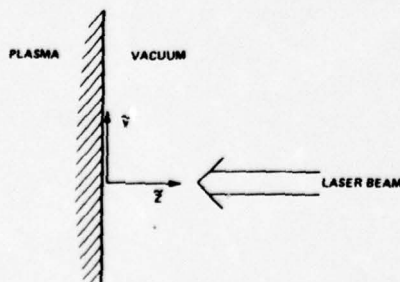


FIG. 1. Laser irradiation of a plasma at a plasma-vacuum interface.

It should be noted that under some conditions (high heating rates and low enough densities), the electrons are not collisionally coupled to the ions. In this case the heating wave represents electron heating with ions remaining cold, and the temperature to be discussed must be interpreted as the electron temperature.² In the analysis to be described, the equations for the axisymmetric case are solved in a fashion similar to that described by Rehm,¹ and a two-dimensional heating wave is calculated analytically.

If the heating takes place very rapidly, then early in the interaction the density remains constant at its initial value $\tilde{\rho}_0$ while the velocities in the axial and the radial directions remain essentially zero. The interface between the plasma and vacuum is at the plane $z = 0$ with the plasma occupying the region $z \leq 0$ (see Fig. 1). Under these conditions the equations describing the plasma heating and the laser radiation absorption are

$$\begin{aligned} \tilde{S}_t &= I\tilde{k}/\tilde{\rho}_0\tilde{T}, & I_t &= -kI, \\ \tilde{p} &= \tilde{\rho}_0\gamma \exp(\tilde{S}/C_v), & \tilde{p} &= \tilde{\rho}_0 R\tilde{T}, & \tilde{k} &= a\tilde{\rho}_0^2/\tilde{T}^{3/2}. \end{aligned} \quad (1)$$

Here, \tilde{z} is the distance measured in the axial direction, \tilde{y} is the distance measured in the radial direction, \tilde{t} is time, \tilde{S} is the entropy per unit mass, \tilde{k} is the absorption coefficient, $\tilde{\rho}_0$ is the density, \tilde{p} is the pressure, R is the gas constant, C_v is the constant-volume specific heat, and γ is the ratio of specific heats. The tilde denotes dimensional quantities. In the equation describing the radiation transport, the laser radiation intensity, $I(\tilde{y}, \tilde{z}, \tilde{t})$, has been assumed to propagate parallel to the z axis without refractive, reflective, and scattering effects and re-radiation has been ignored. In the model for the plasma, a perfect gas has been assumed and thermal conductivity has been neglected. The density of the plasma has been taken as subcritical so that reflection and plasma instabilities can be neglected.

These equations can be used to obtain two coupled nonlinear partial differential equations for the plasma temperature and the laser intensity. For convenience, we introduce normalized quantities as follows:

$$T = \tilde{T}/\tilde{T}_0, \quad I = \tilde{I}/\tilde{I}_0, \quad z = \tilde{z}/l_0, \quad t = \tilde{t}/\tau,$$

where \tilde{T}_0 is the initial temperature of the plasma, \tilde{I}_0 is the peak laser intensity at $\tilde{y} = \tilde{z} = 0$, $l_0 = 1/\tilde{k}_0 \equiv \tilde{T}_0^{3/2}/a\tilde{\rho}_0^2$ is the initial absorption length at the laser frequency, and $\tau = \tilde{\rho}_0 C_v \tilde{T}_0 / \tilde{I}_0 \tilde{k}_0$ is the time scale for the initial energy addition by the laser. Equation (1) can be written as

$$T_t = I/T^{3/2}, \quad I_t = -I/T^{3/2}. \quad (2)$$

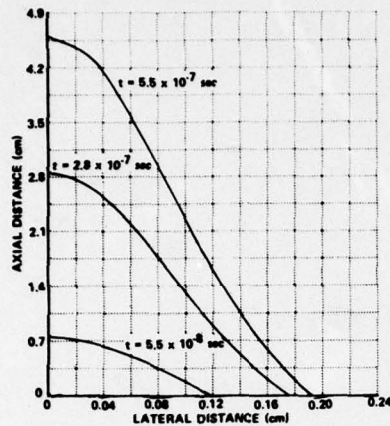


FIG. 2. 10-eV constant-temperature profiles at three times for an axisymmetric bleaching wave. Calculated for a ruby laser of power 10^6 W and focal spot radius 1 mm incident upon a hydrogen plasma of initial temperature 2 eV and initial electron density 1.3×10^{19} cm $^{-3}$. Also for a CO $_2$ laser of power 10^6 W and focal spot radius 1 mm incident upon a hydrogen plasma of initial temperature 2 eV and initial electron density 8.5×10^{17} cm $^{-3}$.

These equations are the same as those obtained earlier by Rehm¹ for the one-dimensional case. If the same technique is used to solve the equations, they can be combined and integrated twice to give

$$\frac{2}{3}T^{3/2} + 2T^{1/2} + \ln\left(\frac{T^{1/2} - 1}{T^{1/2} + 1}\right) = z + g(y, t). \quad (3)$$

When the intensity distribution incident upon the plasma at the $z = 0$ plane is specified, $I(y, z = 0, t) = \Gamma(y, t)$, the function $g(y, t)$ can be determined:

$$g(y, t) = \frac{2}{3}[T(y, 0, t)]^{3/2} + 2[T(y, 0, t)]^{1/2} + \ln\left(\frac{[T(y, 0, t)]^{1/2} - 1}{[T(y, 0, t)]^{1/2} + 1}\right), \quad (4)$$

where

$$T(y, 0, t) = \left[\frac{5}{2} \int_0^t \Gamma(y, t') dt' + 1 \right]^{2/5}. \quad (5)$$

Equations (3)–(5) represent the solution for the bleaching wave in the axisymmetric case. This heating wave is a high-temperature region which propagates (or diffuses) axially into the plasma, the lateral structure being solely due to the lateral structure of the incident pulse. Certain asymptotic features of this wave can be calculated from the solution given in these equations. As a special, representative case, we have taken

$$\Gamma(y, t) = \exp(-y^2/\sigma^2). \quad (6)$$

This functional form represents a laser beam of Gaussian profile with a characteristic length σ in the lateral direction and with an intensity which is switched on at $t = 0$ and remains uniform with time thereafter.

The form of this solution can be simplified when the temperature of the bleaching wave compared with the ambient

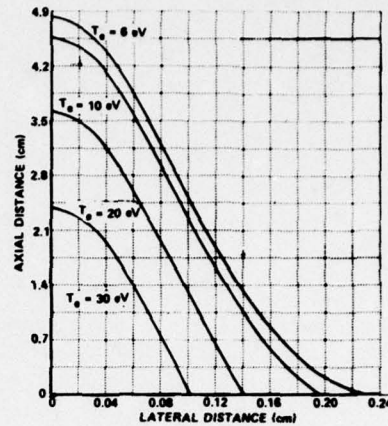


FIG. 3. Constant-temperature profiles at a fixed time of 5.5×10^{-7} sec for an axisymmetric heating wave. Laser and plasma conditions are the same as those given in Fig. 2.

temperature is large, $T \gg 1$, and when the quantity

$$\int_0^t \Gamma(y, t') dt' = t \exp(-y^2/\sigma^2) \gg 1,$$

i.e., late in the interaction and not far from the laser beam axis. Then, the analytical expression for the heating wave can be approximated as

$$z \cong \frac{2}{3}T^{3/2} - \left[\left(\frac{5}{2} \right) t \exp(-y^2/\sigma^2) \right]^{3/5}, \quad (7)$$

and this form for the solution makes calculations of temperature profiles rather easy.

Calculations of constant-temperature contours from Eq. (7) have been made for the axisymmetric bleaching wave. Two sets of conditions have been used to display the constant-temperature contours in dimensional form. They are presented in Figs. 2 and 3. One set of conditions was considered for ruby-laser irradiation and the other for CO $_2$ -laser irradiation. For the CO $_2$ -laser conditions the temperature should be considered to be the electron temperature (the energy-addition time $\tau \cong 5 \times 10^{-10}$ sec and the electron-ion equilibration time⁹ $\tau_{eq} \cong 8 \times 10^{-9}$ sec) whereas for the ruby-laser conditions the temperature will be both electron and ion equilibrated temperature ($\tau \cong 5 \times 10^{-10}$ sec and $\tau_{eq} \cong 8 \times 10^{-11}$ sec). The gasdynamic motions can be expected to become important around 5×10^{-8} sec when the electrons and ions are coupled.

In Fig. 2 the constant-temperature (electron temperature) profile, for $T = 10$ eV at three times during the bleaching wave is shown. The intensity of the laser has a Gaussian profile with respect to lateral distance y as given in Eq. (6). The plots in Fig. 2 show that the heating wave progresses much more rapidly in the axial direction (into the target) than laterally, and the form of the profile has a roughly Gaussian shape. In Fig. 3 plots of four constant-temperature profiles at a fixed time are shown. The temperature is seen to decrease more rapidly in the lateral than in the axial direction.

This research was sponsored by the Air Force Office of Scientific Research (AFOSR), United States Air Force.

- ¹ R. G. Rehm, *Phys. Fluids* **13**, 921 (1970).
- ² L. C. Steinhauer and H. G. Ahlstrom, *Phys. Fluids* **14**, 81 (1971).
- ³ L. C. Steinhauer and H. G. Ahlstrom, *AIAA J. (Am. Inst. Aeronaut. Astronaut.)* **10**, 429 (1972).
- ⁴ J. M. Dawson, A. Hertzberg, G. Vlases, H. Ahlstrom, L. Steinhauer, R. Kidder, and W. Kruer, in *Proceedings of the Esfahan Symposium on Fundamental and Applied Laser Science* (Wiley, New York, 1973), p. 119.
- ⁵ A. Hertzberg, *Proc. IEEE* (to be published).
- ⁶ H. Rutkowski, K. Berggren, and G. C. Vlases, *Bull. Am. Phys. Soc.* **18**, 1293 (1973).
- ⁷ H. G. Ahlstrom and L. C. Steinhauer, *Bull. Am. Phys. Soc.* **18**, 1293 (1973).
- ⁸ G. T. Schappert, *Bull. Am. Phys. Soc.* **18**, 1293 (1973).
- ⁹ L. Spitzer, Jr., *Physics of Fully Ionized Gases* (Interscience, New York, 1956).

Two-dimensional growth of laser-driven waves in a hydrogen free jet

H. M. Thompson, J. W. Daiber, and R. G. Rehm*

Calspan Corporation, Buffalo, New York 14221
(Received 2 October 1975)

A Q-switched ruby laser has been used to irradiate a free jet of hydrogen. The propagation of the luminous wave which originated in the breakdown spark has been monitored using an optical system which permitted simultaneous observation of the motion along and perpendicular to the coincident axes of the focused laser beam and the free jet. Correlation of the luminous frontal wave and the late-time shock wave (made visible with a schlieren system) with the third root of the ratio of laser power to free-jet plenum pressure was found to hold over a range of several orders of magnitude.

PACS numbers: 52.50.Jm, 45.70.Mm, 52.35.Lv

I. INTRODUCTION

Laser irradiation of solids is of current interest for material damage studies and for heating of matter to controlled thermonuclear reaction conditions. The wave motions induced in the target material control the stress distribution which, in turn, determine the damage that the material may suffer. Sequential photographs taken of the laser-induced shock waves indicate that the motions are not spherically symmetric. This work is concerned with the use of streak photography for recording details of the wave motions.

The laser intensities of interest in these studies, and the material response which they generate, lie well beyond the range of linear heat conduction and elastic stress-wave propagation. Instead, the irradiated solid acquires a large energy per unit mass and is subjected to pressures which exceed the material strength by many factors of 10.¹ In these extreme ranges of energy and pressure, it is no longer meaningful to characterize the material as a solid, since the energies involved far exceed the cohesive energy. In analyzing the motion, it is proper to treat the material as though it were an inviscid fluid, and to replace its constitutive relation by a thermodynamic equation of state.² This approximation, which amounts to using the Euler equations to describe the motion, has been used for many years to treat material response to intense loading under high-speed impact.³ It does not apply, of course, if the irradiation is not sufficiently intense to produce a high-pressure region, and it also fails at sufficiently late time, when the pressure and temperature of the material have returned to levels where features of the solid-state behavior are once again discernible. It does represent a valid and useful approximation, however, during the early period of response to an intense excitation.⁴

The approach taken during the work reported here is to take advantage of the fluid-mechanical nature of the response, by using a gaseous free-jet target to simulate the irradiated solid. There are four major advantages to using a gas as the target rather than a solid. (i) Because of the increased length for the absorption of the laser radiation, the scale of the phenomenon is increased over that in a solid. (ii) The transparency of the gas facilitates the diagnostic procedures. (iii) Because the target densities are lower, higher energies per particle can be obtained for a given laser system. (iv) The re-

servoir density, as well as the laser power, can be varied between experiments so that the dependence of the growth velocities upon both target density and laser intensity can be examined. Other investigators have also found the gaseous free jet a valuable target for interaction studies.^{5,6}

The experimental data presented constitute an extension of our previous⁷ hydrogen free-jet work in three areas. First, the power absorbed in the plasma was measured and the correlation extended to optically thin plasma. Second, the plenum pressure has been extended from 7 to 60 atm, where the plasma density is higher than the critical value for the ruby-laser frequency. Third, the lateral growth of the plasma in a direction perpendicular to the axis of irradiation has been measured at times near the end of the laser pulse. As a result of the lateral growth measurements, it is observed that the plasma fills a shallow cone angle which is never more than 0.4 of the lens focal angle. Therefore, it does not follow the lens focal volume as in laser-induced ambient gas breakdowns.⁸ A possible explanation for the restriction of the plasma is the creation of spontaneous magnetic fields.

Section II describes the laser and recording equipment. This is followed by data on the axial growth of luminosity and the axial shock-wave growth. The lateral shock-wave growth and a description of the optical relay scheme are then presented. Based on the experimental data a heuristic model of the shock-wave growth is given in Sec. VI.

II. LASER SYSTEM AND EXPERIMENTAL PROCEDURE

For these experiments a Pockels cell Q-switched ruby oscillator is used. The rod is 4-in. long and $\frac{3}{8}$ in. in diameter with flat cut ends. A three-etalon resonant reflector is used as the output coupler of the oscillator. This reflector provides a beam divergence for the oscillator of less than 0.5 mrad. The beam then passes through two additional ruby rods each providing an amplification of from 2 to 5. These $\frac{3}{8}$ -in.-diam rods have Brewster cut ends and have a tip-to-tip length of $\frac{9}{16}$ in. The output beam of the laser system is elliptical. The average beam divergence of 1.5-mrad full angle was measured by using various elliptical apertures in front of a calorimeter at the same position as the focusing lens would be located.

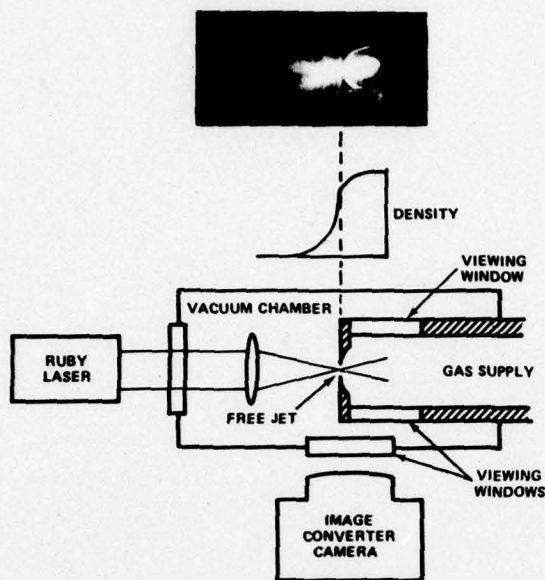


FIG. 1. Composite picture of the early-time data. A schematic of the free-jet apparatus is shown in the lower portion of the figure. At the center the calculated density profile is shown. At the top a time-integrated photograph of the luminous plasma in hydrogen is shown.

The laser beam enters a vacuum chamber where the free-jet apparatus is contained. Gas is admitted into the reservoir chamber 5 msec before the laser is fired. A Kistler type 603L pressure transducer monitors the reservoir pressure and is used to insure that a pressure equilibration occurs before the laser is fired.

The gas escapes from the reservoir through a 2-mm-diam orifice located on the reservoir wall facing the laser beam. The orifice is sharp edged with the throat at the vacuum side of the end wall. In Fig. 1, a schematic diagram of the experimental apparatus is shown; above this diagram is a plot of the axial density profile of the gas as it passes through the orifice. The density along the axis of the jet decreases rapidly from its value in the reservoir; at 4 mm in front of the orifice the density is down by almost two orders of magnitude from the plenum value. The maximum velocity of expansion of gas within the free jet is about two orders of magnitude less than the axial plasma growth during laser heating.

The laser beam is focused into the free jet nearly 2 mm before the orifice with a biconvex lens of focal length 61 mm. A helium-neon laser beam which had been adjusted to have a beam divergence of 1.5 mrad, the same as the ruby laser beam, was used to determine that the diameter of the focal spot conforming to one-half of the peak intensity was 80μ . The laser intensity on target was varied from 4×10^{12} to 1.1×10^{13} W/cm² by changing the peak laser power. When the laser was fired, breakdown occurred and a luminous plasma propagates through the orifice and back into the reservoir chamber. A photograph of the free jet showing the

time-integrated luminosity of the plasma formed during irradiation is in the upper part of Fig. 1.

III. EARLY-TIME LUMINOUS PLASMA GROWTH IN THE AXIAL DIRECTION

The plasma growth was monitored with an image-converter camera operating in the streak mode. When the laser was fired, breakdown occurred in the supersonic stream of gas at a distance of several millimeters from the orifice. As the laser fed energy into the plasma, the plasma expanded and a luminosity front rapidly propagated through the orifice and into the reservoir chamber.

Data on the axial growth velocity into the reservoir were taken over a range of reservoir pressures and laser powers in hydrogen gas. It was found that the luminous front velocities could be correlated by the ratio of absorbed power to gas pressure. This same correlation was used previously for the luminous front growth in air.⁷ With air, however, all the incident radiation was absorbed by the plasma. In hydrogen, particularly at the lower pressures, a significant fraction of the incident radiation was transmitted by the plasma. This is the case for the diamond data of Fig. 4 in Ref. 7. When the peak power was reduced by the measured transmitted power, then the hydrogen data could be correlated.

Additional data has now been taken over the range of reservoir pressures from 4 to 60 atm. The target density at the higher pressures is calculated to be 1.6×10^{21} molecules/cm³. Assuming complete ionization, the plasma electron densities are twice as large. Thus, the electron density has been varied from below to above the critical density (2.3×10^{21} electrons/cm³) required for a plasma frequency to be resonant with the ruby-laser frequency (4.32×10^{14} Hz).

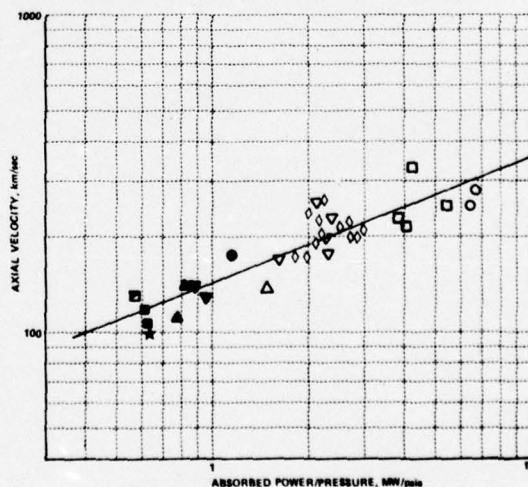


FIG. 2. Measured luminous-front velocities on the axis of a free jet in hydrogen. The symbols indicate the pressure (psig) in the jet reservoir: \circ , 50; \square , 60; \diamond , 90; ∇ , 120; \triangle , 285; \bullet , 385; ∇ , 485; \triangle , 585; \star , 685; \blacksquare , 785; \boxplus , 885.

The experimental results are plotted in Fig. 2. The uncertainty in the axial velocity measurements increases at the higher pressures due to the smaller spatial extent of the plasma growth. A least-squares fit of a straight line to the data yields the correlation

$$V = 10^4 (P/p)^B,$$

where $A = 2.16 \pm 0.6\%$ and $B = 0.39 \pm 9\%$. V is the axial velocity in km/sec, P is the laser power in MW, and p is the plenum pressure in psia. This curve is plotted in Fig. 2. The exponent is predicted to be $\frac{1}{3}$ by a gas-dynamic-type model commonly called the deflagration model.^{2,9} The fit of these data to such a model is quite good. These hydrogen results indicate that the deflagration model describes the interaction process for conditions where nearly none of the incident laser energy is absorbed and for conditions where the electron density in the breakdown plasma exceeds the critical value.

IV. AXIAL SHOCK-WAVE GROWTH OBSERVED AT LATE TIMES

A shock wave is expected to depart from the hot luminous plasma. It is desirable to view this shock wave to understand the coupling of energy from the directly heated region to late-time wave motions in a gas or solid target. The most direct method of observing shock waves in a gas is to use a schlieren system, which monitors the refractive index change associated with the shock wave.

The schlieren system that was employed required the construction of a light source with constant irradiance. This source utilizes a coaxial capacitor with the discharge confined to a channel 1 mm in diameter by 14.5 mm long. The capacitor is a barium titanate coaxial transmission line that has a capacitance of 0.02 μ f. The source is symmetrically constructed with the arc channel coaxial with the grounded return current sheath. The operating voltage is nominally 20 kV, which results in a square current pulse with a jitter in starting of less

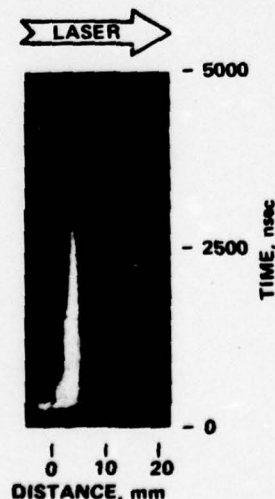


FIG. 3. Streak photograph of laser-induced shock-wave growth in a free jet of hydrogen. The reservoir pressure is 6 atm. The laser peak power is 132 MW and the laser pulse contains 5 J of energy.

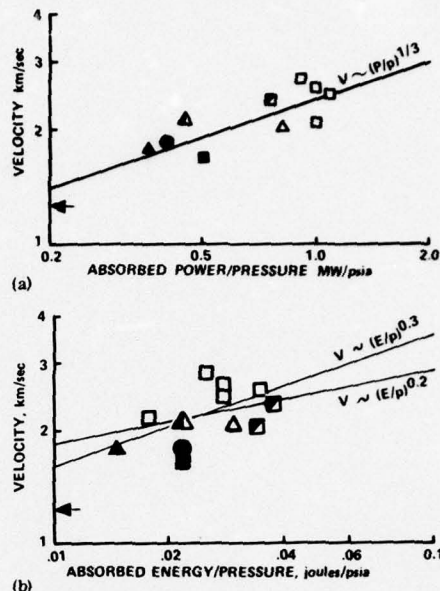


FIG. 4. Measured axial shock-wave velocities in hydrogen. The symbol filling indicates percentage of incident energy absorbed: filled symbols 20%; half-filled symbols, 80%; open symbols, 100%. Symbol shape indicates reservoir pressure (psig): \square , 90; \circ , 115; Δ , 130. The arrow indicates the sonic velocity.

than 0.5 μ sec. The usual gas fill is argon at 1 atm pressure. The lamp output is of nearly constant intensity for time durations up to 3 μ sec.

For the schlieren system, the light emitted on axis is collimated by a 3-in.-diam mirror of 18-in. focal length. The light source is not imaged on an aperture first because the confining effect of the capillary in the source has proven effective in limiting radial growth and giving a satisfactory source diameter. The source is of sufficient brightness that usable streak records have been obtained using 1.5-mm-wide slits at a writing rate of 25 mm/ μ sec on the STL image-converter camera.

A streak record of the shock-wave propagation from its origin into the high-density gas reservoir is shown in Fig. 3. This record was obtained in hydrogen with a reservoir gas pressure of 6 atm and using a laser pulse of 132-MW peak power and a total energy of 5 J. The duration of the sweep for the streak photograph was 5000 nsec.

At early times the camera's photocathode is saturated by the luminous plasma. This saturation was considerably reduced by placing a neutral-density filter of density 1.0 over a portion of the scan slit. The vertical edge of luminosity at 2 mm is the result of this filter. The trajectory of the shock wave is a continuation of that of a luminous front that is seen to separate from the main plasma after termination of the laser heat pulse. The average velocity of the shock wave is substantially less than that of the luminous front. The shock-

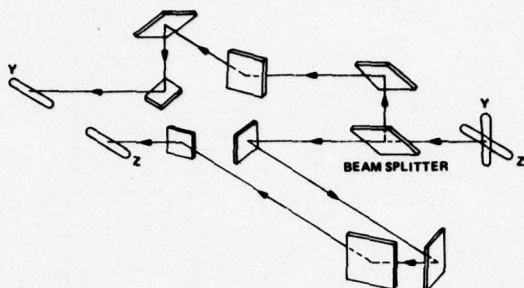


FIG. 5. Schematic diagram of optical system for simultaneous measurement of longitudinal and lateral plasma growth.

wave velocity was read at 1 μ sec after breakdown. For this record the velocity is approximately 1.75 km/sec (Mach 1.4).

The shock-wave velocity has been recorded over a range of laser powers and energies at various hydrogen gas densities. The laser pulse width was increased from 30 to 50 nsec without increasing the laser power so that a comparison could then be made between the correlation of shock-wave velocity with absorbed energy and with absorbed power. The measured shock-wave velocities were plotted against the ratio of absorbed power divided by reservoir pressure and against the ratio of absorbed energy divided by reservoir pressure. Straight lines were fitted to the data. For the power correlation, it was found that the slope was $0.31 \pm 30\%$. Whereas for the energy correlation, the slope was $0.30 \pm 50\%$.

The data is shown in Fig. 4. The power correlation is shown in the upper part of the figure. The straight line has the calculated intercept for best fit but has been plotted with a slope of 0.33. This is the variation predicted by the deflagration model. In the lower part of the figure the energy correlation is shown. Here two lines are plotted. One is the calculated best fit and other has a slope of 0.2 which would be predicted by a spherical blast wave theory. For the present data, it appears that the shock-wave velocity is best correlated with the absorbed power. This observation is somewhat surprising since it might be expected that the late-time shock-wave velocity would scale with the blast-wave theory.

V. SIMULTANEOUS AXIAL AND TRANSVERSE PLASMA GROWTH

The laser-driven plasma not only expands along the laser optical axis, but it also expands in directions perpendicular to the axis. The study of this lateral expansion is important for the interpretation of the present experiment since the decay of the axial velocity will be controlled by loss of energy to lateral expansion. In addition, the extent of cratering or spallation in a solid depends on the three-dimensional stress variation into which the shock wave decays.

An optical system which permits the simultaneous measurement of longitudinal and lateral plasma growth on our image-converter camera has been used to study

two-dimensional growth during laser energy addition. This system, utilizing mirrors, prisms, and a beam splitter, was installed between the test region and the horizontal slit defining the camera image.

A functional schematic of this system is shown in Fig. 5. For simplicity, all surfaces except the beam splitter are shown as mirrors. A vertical slit Y, which views the reservoir directly behind the orifice plate, and a horizontal slit Z, which views the axial region from in front of the orifice to well behind it, are shown on the right-hand side of this diagram. The images of these reservoir regions are optically rotated as shown with the beam splitter and mirrors and imaged adjacent to each other on the scan slit plane of the image-converter camera. In this fashion, streak photographs of both the lateral and axial growth of the plasma during the laser energy addition are obtained simultaneously.

Figure 6 shows a photograph of the gas reservoir with the vertical and horizontal slits backlit. Photographs of this type were used for alignment purposes. The relative position of the vertical image of the slit is easily adjusted to any location along the axis by translating the appropriate mirror.

A schematic diagram of the free-jet orifice with the axial (Z) scan slit and the lateral (Y) scan slit is shown in Fig. 7. Also shown on this figure is a record of the axial plasma growth and the lateral plasma growth; as described above, these records were taken simultaneously on a single streak photograph. For this run the plenum pressure of hydrogen was 5 atm and the incident peak power was 300 MW.

A typical axial-growth record shows the plasma starting early in the laser pulse in the low-density part of the gradient and growing rapidly through the jet orifice into the reservoir. After termination of the laser pulse, the luminous region growth is much slower. The lateral growth is viewed at a point inside the reservoir near the jet orifice. Generally, the location of the viewing station corresponds to a time near the end of the laser pulse.

Distance-time plots of the luminous-front growth read from streak records have been made. The axial growth of the luminous region at the time immediately after the laser pulse has been found to grow with time as $t^{0.2}$. This growth is the same as that measured by ourselves and others for axial growth in an ambient-gas laser-produced spark.⁹ This growth is less rapid than that predicted from spherical blast-wave theory ($t^{0.4}$). The lateral plasma growth after termination of the laser

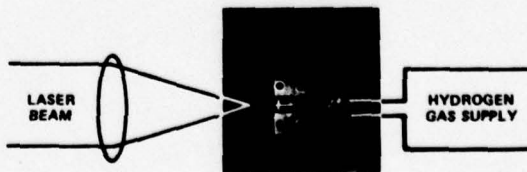


FIG. 6. Photograph of gas reservoir with the horizontal and vertical scan slits for the image-converter camera backlit.

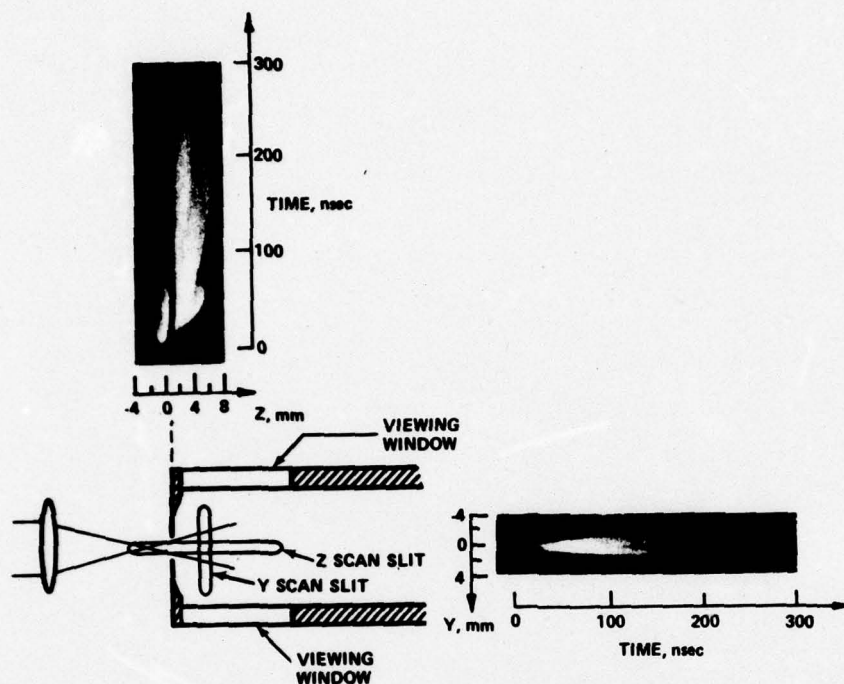


FIG. 7. Axial and lateral growth records in hydrogen at 5 atm reservoir pressure. The incident laser power is 300 MW.

pulse has been found to increase somewhat faster with time ($t^{0.6}$) than that predicted by cylindrical blast-wave theory ($t^{0.5}$).

An average lateral-growth velocity was measured at about 60 nsec after breakdown and, therefore, represents the lateral growth of the luminous region after termination of the laser pulse. This velocity is about a factor of 30 below the axial growth during laser irradiation. It should be noted that during the time of this record, the lateral expansion in the free-jet plenum is not influenced by the plenum walls. The maximum lateral velocities observed would require more than a microsecond to reach the wall and a sonic wave would require over a millisecond to reach the wall.

The lateral location of the plasma was measured from the streak photographs and compared to the extent of the light cone filled by laser radiation in the absence of hydrogen breakdown. The extent of this irradiated region along the Y scan slit is indicated in Fig. 7. For all cases, the plasma filled a region only one-half of the lateral extent available to it. The fact that the plasma expanded axially and not laterally was used in the model described below to explain the correlation of shock-wave velocity with laser power. Why the plasma expands one dimensionally is not known from the present data. A possibility, however, is the recently observed spontaneous magnetic fields created in laser matter interactions.¹⁰ A program to examine the free-jet plasmas for such fields is currently being carried out.¹¹

VI. LATE-TIME GROWTH MODEL

A model of the late-time shock-wave process was

formulated, which appears to correlate the experimental results obtained for luminous growth velocity and shock-wave velocity in the axial direction. This model assumes that, at the time of laser termination, the heated gas, which is at a high temperature and pressure, resembles a cylinder that is surrounded by a cool low-pressure gas. The high-pressure plasma thus creates a strong shock wave everywhere on its surface. The strength of this shock wave can be calculated from the shock-tube equations.¹² As the shock wave propagates away from the surface, there is a rapid adjustment in strength as the system adjusts to the finite size of the laser-heated region. After this the shock-wave strength decays in an inverse manner with its increasing area. With this model, the late-time shock-wave strength is directly proportional to the initial shock-wave strength. The shock-tube equations predict that this initial strength is proportional to the sound speed in the driver.

The early-time data indicates that the deflagration model is applicable to the interaction process. One of the consequences of this model is that the sound speed in the heated plasma is directly proportional to the frontal velocity or to the ratio of absorbed power divided by pressure to the $\frac{1}{2}$ power. Thus, the late-time shock-wave strength should scale with this same parameter.

Calculations have been made on the basis of this model of the axial trajectories of the luminous front during heating and of the shock wave after heating. In the present experiments, the thermodynamic state of the heated plasma is not measured; therefore, the deflagration model was used to predict the effective driver sound speed. The decay of the shock-wave strength was calculated on the basis of a spherical blast wave. For that

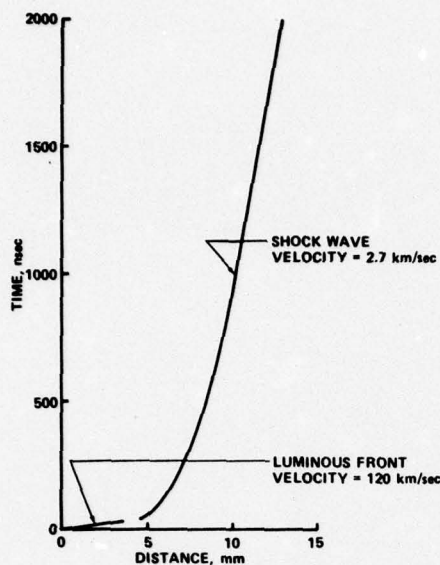


FIG. 8. Calculated luminous-front and shock-wave trajectories in hydrogen.

portion of the shock-wave front on the axis, this should give a reasonable representation. The time history of the shock wave as it adjusts to the driver size was neglected and only the final strength was estimated. The result of this series of calculations is shown in Fig. 8.

Straight lines were fitted to the calculated trajectory at early times and at 1 μ sec after initiation. The slopes of these lines yielded a velocity which could be compared to measurements. These velocities, as well as the shock wave location, agreed with the observed data to within 10%. Direct measurements of the temperature and/or density in the laser-heated plasma would serve to remove much of the uncertainty.

VII. CONCLUSION

Scaling of the plasma growth with the laser intensity and the plenum density has been obtained with hydrogen targets over a wide parametric range extending from optically thin plasmas to overdense plasmas. The axial velocity during laser heating and the average lateral velocity after the laser pulse have been found to scale

with the parameter of intensity over density to the $\frac{1}{2}$ power. Such scaling is consistent with a model in which the laser heats a cylindrical slug of plasma as in a one-dimensional deflagration process. Subsequent expansion is governed then by the temperature to which the plasma slug has been heated during laser energy deposition. As a result, the velocities vary with the absorbed power and not laser energy.

The relation of these findings to the dynamic behavior of laser irradiated solids requires further analysis. However, several general statements can be made. Strong shock waves in a target will be created. The strength of the shock wave will, for short duration laser pulses, depend on peak power and not on total pulse energy. That fraction of the incident laser energy which is not absorbed because of target transparency or, presumably, because of reflection and scattering should be excluded in estimating shock strength. During the laser irradiation the growth of the shock wave will be primarily one-dimensional along the laser optical axis. Lateral expansion will proceed at a much lower rate.

ACKNOWLEDGMENTS

This research was sponsored by the Air Force Office of Scientific Research (AFSC) United States Air Force. The authors would like to thank Dr. W.J. Rae for the many suggestions he made during the course of this program.

*Present address: Mathematical Analysis Section, IBS, National Bureau of Standards, Washington, D.C. 20234.

¹C.G.M. Van Kessel and R. Sigel, *Phys. Rev. Lett.* **33**, 1020 (1974).

²R.S. Cooper, *AIAA J.* **11**, 831 (1973).

³W.J. Rae, *High-Velocity Impact Phenomena*, edited by R. Kinslow (Academic, New York, 1970), Chap. 6.

⁴R.G. Rehm, *Phys. Fluids* **13**, 921 (1970).

⁵H.J. Neusser, H. Puell, and W. Kaiser, *Appl. Phys. Lett.* **19**, 300 (1971).

⁶T.K. Chu and L.C. Johnson, *Phys. Fluids* **18**, 1460 (1975).

⁷H.M. Thompson, R.G. Rehm, and J.W. Dalber, *J. Appl. Phys.* **42**, 310 (1971).

⁸J.W. Dalber and H.M. Thompson, *Phys. Fluids* **10**, 1162 (1967).

⁹C. Fauquignon and F. Floux, *Phys. Fluids* **13**, 386 (1970).

¹⁰J.A. Stamper, K. Papadopoulos, R.N. Sudan, S.O. Dean, E.A. Mclean, and J.M. Dawson, *Phys. Rev. Lett.* **26**, 1012 (1971).

¹¹H.M. Thompson and J.W. Dalber, *American Physical Society Meeting*, 1975 (unpublished).

¹²H.W. Liepmann and A. Roshko, *Elements of Gasdynamics* (Wiley, New York, 1957).

Section IV

ELECTRON-TEMPERATURE AND SPONTANEOUS MAGNETIC FIELD MEASUREMENTS IN A LASER-IRRADIATED FREE JET

H.M. Thompson and J.W. Daiber
Calspan Corporation, Buffalo, New York 14221

The output of a Q-switched ruby laser irradiated a freely expanding jet of nitrogen gas. The laser optical axis was collinear with that of the jet. Gaseous breakdown occurred and the remaining energy within the laser pulse heated the plasma and drove forward-travelling waves through the orifice and into the plenum of the jet. The temperature of the electrons within the plasma was measured using relative transmittance of x-rays through thin metal-foil spectrometers. The temperature varied as the square of the wave velocity from 60 eV to 160 eV. Measurements were also made of the spontaneous magnetic fields generated in the vicinity of the plasma.

INTRODUCTION

The interactions which occur when a high-intensity laser beam irradiates a gaseous free jet are of interest because the process offers a simple simulation of some of the phenomena occurring in laser-heated pellet implosions for fusion,¹ in laser-heated cylindrical plasmas for fusion,^{2,3} and in laser-generated target impulses.⁴ The basis of the simulation is that, for a range of energy addition rates, such as used in the present experiments, the targets can all be treated as inviscid fluids. For lower rates, the cohesive energy of the target is significant. For higher rates, nonlinear electromagnetic interactions and additional transport processes are significant. The advantages of the free-jet target are the long scale length for the interaction, the transparency of the gas, and the variability of target density as well as laser intensity.

Our previous results are summarized in Refs. 5 and 6. The data reported herein complete this work by showing that the temperature characteristic of the processed gas increases as the square of the velocity with which the luminous front expands, which is in accord with predictions based on a gas-dynamic model. Measurements are also reported of the spontaneous magnetic field which is generated during the laser irradiation of the plasma and which persists for some time thereafter. The strength of this azimuthal magnetic field is large enough to retard the lateral growth of the plasma.

DESCRIPTION OF APPARATUS

The characteristics of the Q-switched ruby laser and the free-jet target are the same as described in detail in Ref. 6. The free jet consisted of a plenum filled with gas at a relatively high pressure. This gas expanded through a 2-mm-diameter orifice into a vacuum chamber. Within an orifice diameter, the density along the centerline of the jet has fallen by a factor of ten. The laser was operated with peak powers of 200 to 500 MW with pulse durations (FWHM) from 15 to 25 ns. The laser beam was focused to an 80- μ m diameter spot 1 to 2 mm from the orifice in the expansion. The laser optical axis was coaxial with the jet centerline as depicted in Fig. 1.

Laser energy addition to the gas has been shown⁵ to drive luminous waves into the target and not back towards the focusing lens. During the program, the free-jet plenum which was fabricated of metal was replaced by one fabricated of lucite. This was done to minimize perturbation to the magnetic field due to alterations of the return-current path which could occur with a conducting housing.

The x-ray emission from the plasma was detected by monitoring the fluorescence induced in an NE 102 plastic scintillator with RCA 8575 photomultiplier tubes.⁸ A 1/8-inch-thick aluminum plate (approximately 860 mg/cm²) with a 3/8-inch-diameter aperture cut in it was placed over the scintillator on the plasma side to limit the photon flux reaching the photocathode, thereby preventing nonlinear operation of the photomultiplier tube. Two detectors were utilized:

one with a 7.0 mg/cm^2 foil of aluminum, the other with a 23.1 mg/cm^2 foil of beryllium placed between the aperture plate and the scintillator. The thin metal foils filtered the x-ray flux emitted by the plasma. By assuming that the radiation is characteristic of free-free Bremsstrahlung, the determination of a plasma temperature⁹ from the ratio of fluxes in the two wavelength intervals¹⁰ can be made. The thin foils were sufficiently thick that, based on our previous measurements, detectable line radiation would not be transmitted. The uncertainty in the computed temperatures is $\pm 8\%$ and is determined by the error in reading oscilloscope records.

The azimuthal magnetic fields were detected using inductive probes.¹¹ The coils in these probes were made from #42 wire wound in 2 layers to internal diameters of 0.125 mm with 40 turns, 0.05 mm with 20 turns, and 1.0 mm with 10 turns. The coils were encased with epoxy on the tip of 2-mm diameter tubing. Electrostatic shielding and a 50- Ω coaxial signal cable were also built into the probe. Care was taken in fabrication¹² of the probe to obtain an impedance match to the signal cable and to maintain a constant impedance to within 5% over the frequency range of interest.

The electrical output of the probe is proportional to the time derivative of the magnetic field which penetrates it. The proportionality constant is the effective product of the number of turns in the coil and the area of the coil. The magnetic field was obtained by integration of the probe signal with a simple, passive RC integrator having a time constant of 198 ns. This time constant is nominally ten times the quarter cycle duration of the first peak in the magnetic-field derivative signal.

The effective coil area was determined by placing the probe in the spatially uniform field¹³ at the midpoint of a Helmholtz coil. The Helmholtz coil was excited by either a cw oscillator to determine the natural resonant frequencies of the probe system or a 10 ns rise time pulse to determine directly the effective probe area over the desired bandwidth.¹⁴ Because of the distributed capacitance of the probe system, the calibration required the use of the same cables, bulkhead fittings, terminations, coaxial adaptors, and integrator circuits exactly as they were used in the free-jet experiments.

The coil axis of the probe was orthogonal to the laser optical axis. Three probes were positioned on the vacuum side of the free jet, and three were positioned within the high-pressure plenum. Previous work has shown that the plasma generation is sufficiently symmetric that angular variations in the field strength at a fixed radius do not occur.¹⁵ Therefore, the probes were placed at different azimuthal positions to minimize interference. The probes were also placed at three radial distances from the centerline to measure the radial variation of the field strength simultaneously for each test plasma.

TEMPERATURE MEASUREMENT

The one-dimensional gasdynamic model which describes the interaction of an intense light beam with a target was first proposed by Fauquignon and Floux.¹⁶ This model considers the absorbed laser energy to act as a chemical heat release behind a deflagration wave which is being driven into the target. Propagating ahead of the deflagration wave is a shock wave. Behind the deflagration wave is an isothermal expansion of hot target material into the ambient vacuum. The model predicts that the velocity with which the deflagration wave propagates into the target should vary as the ratio of laser intensity I to target density ρ raised to the $1/3$ power. Previous measurements with solid targets¹⁶ and with gaseous targets⁶ (in which both I and ρ were varied) have verified this scaling law.

The model also predicts that the temperature of the gas in the expansion should vary as wave-velocity squared. Verification of this was obtained for solid targets,¹⁶ but measurements for gaseous targets have not as yet been reported. Such data are needed to substantiate the applicability of the deflagration-wave model to the free-jet interaction.

The metal-foil absorption spectrometer used in the present experiments to infer the temperature could only sense x-rays emitted by the plasma in the laser-induced isothermal expansion. The temperatures found varied from 70 to 160 eV. The variation of the temperature with the velocity of the luminous

wave which propagated into the plenum is shown in Fig. 2. Data were obtained for peak laser powers from 200 to 400 MW and for plenum pressures from 10 to 95 psia. A least-squares fit of the data shown in Fig. 2 indicates that temperature varies with velocity as

$$T = 10^{-a} V^b$$

where $a = 2.4 \pm 0.6$ and $b = 2.0 \pm 0.3$, with T in eV and V in km/s. Thus, the variation anticipated from the gasdynamic model is verified.

MAGNETIC-FIELD MEASUREMENTS

The objective of the initial experiments was to establish the validity of the magnetic-probe signal. A test series was run using a 0.003-inch-thick mylar foil as the target. The dB_ϕ/dt time history and its magnitude were in agreement with that obtained elsewhere on mylar targets.¹⁷ Tests were also carried out to verify that the probe voltages were not due to high-energy photons, RF noise, or electrostatic fields.

The free-jet experiments utilized nitrogen as the target gas. A copy of the magnetic-field probe output for a run which had the metallic free-jet housing with a plenum pressure of 40 psia and a laser peak power of 360 MW with a pulse duration of 16 ns, is shown in Fig. 3. In preparing this figure, it was assumed that the magnetic field appeared simultaneously with the laser-induced plasma.¹⁸ This particular probe had an effective area of $6.5 \times 10^{-6} \text{ m}^2$ and was positioned 4.0 mm before the orifice at 5.0 mm from the centerline. In this test series, this was the only probe placed outside the plenum which could sense the azimuthal magnetic field. The signal shows a rise time of 30 ns which lags the 16 ns rise of the laser field. Since the probe accurately reproduced a magnetic field which rose in 10 ns during calibration, it must be inferred that the observed response is due to the finite rise time of the magnetic field in the plasma. The maximum azimuthal magnetic-field strength obtained from the integrator was 33 G. The polarity of the field indicates that it was created by a current on the free-jet axis which is flowing into the plenum.

Tests similar to this were carried out for several laser powers P and plenum pressures p . The reduced data are shown in Fig. 4 as the open symbols with the vertical bar. For all these runs breakdown first occurred 1.4 ± 0.2 mm before the orifice plate. The variation of magnetic-field strength with P/p was found by a least-squares fit to be

$$B_{\theta} = 10^a (P/p)^b$$

where $a = -0.6 \pm 0.1$ and $b = 2.0 \pm 0.1$, with B_{θ} in G and P/p in MW/psia. This equation is plotted in Fig. 4 with short dashes. The data could have been influenced by the nearness of a conducting plane in the form of the orifice plate. Therefore, a nonconducting free-jet housing was fabricated out of lucite and the experiments repeated.

The variation of the azimuthal magnetic-field strength at a fixed distance of 1.8 mm in front of the orifice for the lucite housing is shown in Fig. 4 as a function of the ratio of laser power to plenum pressure. Three sets of data are shown. The filled symbols are for runs in which the laser was focused so that breakdown occurred 1.4 ± 0.2 mm before the orifice. The open symbols are for runs in which the focusing lens was moved back so that breakdown occurred 2.2 ± 0.2 mm before the orifice. A large change in magnetic-field strength is observed as the location of breakdown relative to the probe is varied. This also occurs with laser-irradiated solid targets. Both sets of data were for the probe at 5.5 mm from the centerline. At this location, the magnetic field reached peak strength at times the order of 100 ns after breakdown.

A least-squares fit to the data shown with filled symbols indicates that magnetic-field strength varies as

$$B_{\theta} = 10^a (P/p)^b$$

where $a = 0.60 \pm 0.03$ and $b = 0.39 \pm 0.03$. This dependency of B_{θ} on the ratio (P/p) is much weaker than that indicated by the earlier data obtained with the metallic housing.

The radial dependence of the magnetic field was determined by probes situated a distance of 9.6 mm, 5.5 mm, and 4.0 mm from the centerline. Data obtained with the close-in probe for breakdowns occurring 1.4 ± 0.2 mm before

fit of the data again indicates a slope near $1/3$.¹⁹ However, the standard deviation of the straight-line fit to the data is now ± 0.09 , which is approximately three times that determined from the data collected farther from the plasma. The radial dependence indicated by these averaged curves is radius to the inverse 1.7 power. Individual runs indicate variations in magnetic-field strength between these two radial stations which vary as radius to the inverse square (as observed in Ref. 20) to near independence of radius. Those tests which indicated the steeper variation in magnetic-field strength were also the tests for which the plasma temperature was greater than 100 eV. For all runs, the magnetic-field strengths measured on the two more-distant probes were consistent with the inverse 1.7 power dependence on radius.

Selecting those tests for which the radial dependency of the magnetic-field strength was as radius to the 1.7 power for all three probe locations, an extrapolation was made to a radial distance corresponding to the lens focal radius. Such an extrapolation suggests that azimuthal fields approaching a megagauss²¹ are generated by the large currents within the plasma. The magnetic pressure associated with such fields is equivalent in magnitude to the kinetic pressure within a plasma with a density near an amagat and a temperature near 100 eV. Consequently, the lateral expansion of the plasma will be inhibited during the time such fields exist. The lack of lateral expansion has, in fact, been reported,⁶ and thus provides indirect evidence of the existence of such large magnetic fields.

The probes located within the high-pressure plenum showed a magnetic-field strength which was approximately $1/20$ of that measured external to the plenum. The reason for this is thought to be associated with the short mean-free-path of the high-energy photons which are emitted by the hot plasma. These photons photoionize the ambient gas and thereby create a return current sheath for the laser-generated current. At higher pressures, the photon mean-free-path decreases,¹⁸ forcing the return current sheath to be mainly within the region defined by the radial distance to the probes. Consequently, the probe coils are partially shielded from the axial current flow.

One additional experiment was carried out with the lucite housing to make a direct measurement of the axial current flow²² associated with the azimuthal magnetic fields. A 3-mm-internal-diameter, 15-turn toric coil (Rogowski coil) was placed concentrically around the free-jet orifice. The signal from the Rogowski coil corresponded to peak axial currents of 200 A flowing into the free-jet plenum. The data indicate that the current varies as the ratio P/p to the $1/3$ power; however, because of the limited range of test conditions, the confidence in this scaling relation is not high. For these runs, a simultaneous measurement of magnetic-field strength could not be obtained because the Rogowski coil shielded the probes. However, from the earlier data at the same test condition, a typical value of magnetic-field strength is 20 G at 5.5 mm from the centerline. The Biot-Savart law can be used to calculate an axial current flow of 55 A at these conditions.²³ This is substantially lower than observed with the Rogowski coil.

SUMMARY

The measured plasma temperatures scaled with the square of the wave velocity, thus lending further support to the validity of the gasdynamic model in describing laser-target interactions over the tested range of laser intensities and target densities. A spontaneously generated azimuthal magnetic field was observed which reached peak value near the end of the laser heating pulse. The strength of the field varied as the ratio of laser power to plenum pressure to a power which depended on whether the housing was or was not conducting. Extrapolation of the data to the surface of the plasma indicated field strengths the order of a megagauss. The existence of such fields indicates that the associated magnetic pressures could restrict the lateral expansion of the plasma.

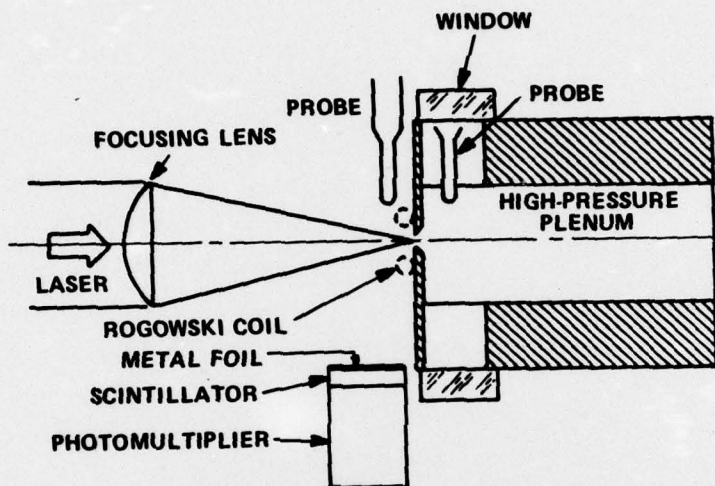
ACKNOWLEDGEMENT

This research was sponsored by the Air Force Office of Scientific Research (AFSC). The authors would like to thank Dr. R.G. Rehm for his many suggestions made during the early phases of this program.

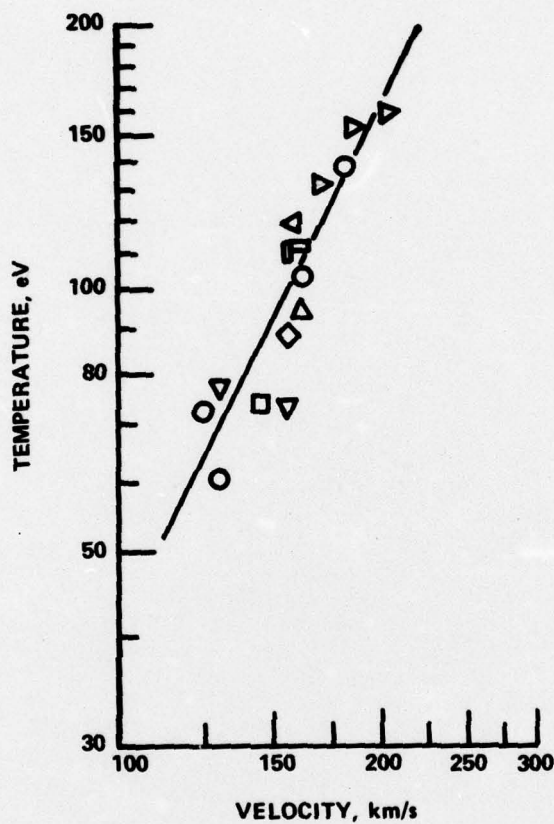
REFERENCES

1. K.A. Brueckner and S. Jorna, "Laser-driven fusion," Rev. Mod. Phys., vol. 46, pp. 325-367, 1974.
2. J.M. Dawson, A. Hertzberg, R.E. Kidder, G.C. Vlases, H.G. Ahlstrom and L.C. Steinhauer, "Long-wavelength high-powered lasers for controlled thermonuclear fusion," 4th Conf. on Plasma Physics and Controlled Thermonuclear Fusion, vol. 1, pp. 673-687, Int'l. Atomic Energy Agency, Vienna, 1971.
3. T.K. Chu and L.C. Johnson, "Measurement of the development and evolution of shock waves in a laser-induced breakdown plasma," Phys. Fluids, vol. 18, pp. 1460-1466, 1975.
4. J.A. Fox, "Effect of pulse shaping on laser-induced spallation," Appl. Phys. Lett., vol. 24, pp. 340-343, 1974.
5. H.M. Thompson, R.G. Rehm and J.W. Daiber, "Laser driven waves in a freely expanded gas jet," J. Appl. Phys., vol. 42, pp. 310-314, 1971.
6. H.M. Thompson, J.W. Daiber and R.G. Rehm, "Two-dimensional growth of laser-driven waves in a hydrogen free jet," J. Appl. Phys., vol. 47, pp. 2527-2432, 1976.
7. J.A. Stamper, K. Papadopolis, R.N. Sudan, S.O. Dean, E.A. McLean and J.M. Dawson, "Spontaneous magnetic fields in laser-produced plasmas," Phys. Rev. Lett., vol. 26, pp. 1012-1015, 1971.
8. J.W. Daiber and H.M. Thompson, "X-ray temperatures from laser-induced breakdown plasmas in air," J. Appl. Phys., vol. 41, pp. 2043-2047, 1970.
9. F.C. Jahoda, E.M. Little, W.E. Quinn, G.A. Sawyer and T.F. Stratton, "Continuum radiation in the x-ray and visible regions from a magnetically compressed plasma (SCYLLA)," Phys. Rev., vol. 119, pp. 843-856, 1960.

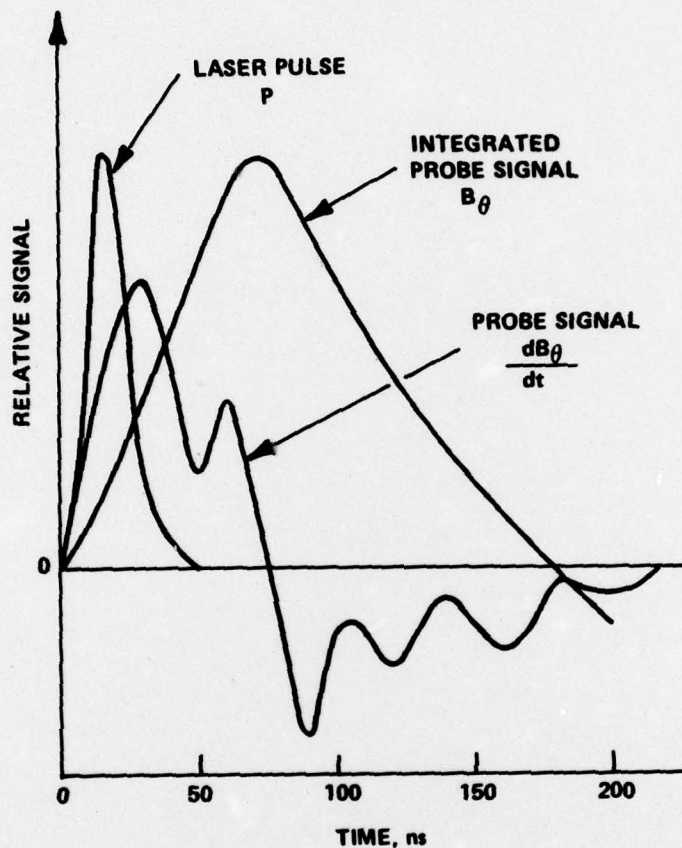
10. R.C. Elton, "Determination of electron temperatures between 50 eV and 100 keV from x-ray continuum radiation in plasmas," Naval Research Lab. Rep. 6738, 11 December 1968.
11. R.C. Phillips and E.B. Turner, "Construction and calibration techniques of high-frequency magnetic probes," Rev. Sci. Instrum., vol. 36, pp. 1822-1825, 1965.
12. S.E. Segre and J.E. Allem, "Magnetic probes of high frequency response," J. Sci. Instrum., vol. 37, pp. 369-371, 1960.
13. J.R. Reitz and F.J. Milford, Foundations of Electromagnetic Theory, Addison & Wesley, pp. 156-157, 1967.
14. B. Wegener, "Measurements of Early Magnetic Fields in Laser Produced Plasma," Naval Postgraduate School, AD-784 763, June 1974.
15. L.L. McKee, R.S. Bird and F. Schwirzke, "Self-generated magnetic fields associated with a laser-produced plasma," Phys. Rev. A., vol. 9, pp. 1305-1311, 1974.
16. C. Fauquignon and F. Floux, "Hydrodynamic behavior of solid deuterium under laser heating," Phys. Fluids, vol. 13, pp. 386-391, 1970.
17. R.S. Bird, L.L. McKee, F. Schwirzke and A.W. Cooper, "Pressure dependence of self-generated magnetic fields in laser-produced plasma," Phys. Rev. A, vol. 7, pp. 1328-1331, 1973.
18. M.G. Drouet, R. Bolton, G. Saint-Hilaire, P. Kieffer, Z. Szili, H. Pépin, B. Grek, A. Thiboudeau and K. Trépanier, "Simultaneous measurements of current and magnetic field in laser-produced plasmas," Appl. Phys. Lett., vol. 29, pp. 469-471, 1976.
19. M.G. Drouet and H. Pépin, "Parametric study of the current induced in a CO₂ laser plasma," Appl. Phys. Lett., vol. 28, pp. 426-428, 1976.
20. R. Serov and M.C. Richardson, "Measurements of intense magnetic fields associated with laser-produced plasmas," Appl. Phys. Lett., vol. 28, pp. 115-118, 1976.
21. J.A. Stamper and B.H. Ripin, "Faraday-rotation measurements of megagauss magnetic fields in laser-produced plasmas," Phys. Rev. Lett., vol. 34, pp. 138-141, 1975.
22. M.G. Drouet and R. Bolton, "Distribution of self-generated current in laser-produced plasmas," Phys. Rev. Lett., vol. 36, pp. 591-594, 1976.
23. R.S. Case, Jr. and F. Schwirzke, "Background gas pressure dependence and spatial variation of spontaneously generated magnetic fields in laser-produced plasmas," J. Appl. Phys., vol. 46, pp. 1493-1498, 1975.



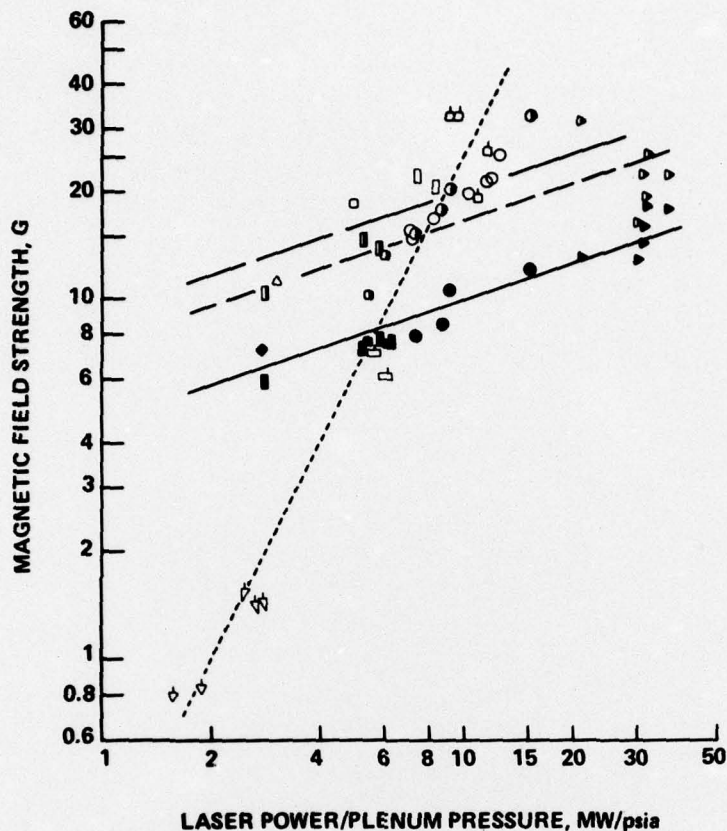
- 1 Schematic diagram of the experiment showing the approximate position of the diagnostics. The Rogowski coil is shown with dashed lines because it was only present for one run series. The probe inside the plenum was at a different azimuthal position from that of the viewing window.



- 2 Variation of plasma temperature with the velocity of the forward propagating luminosity wave. The symbol shape denotes plenum pressure: \circ 10 psia, \triangleright 14 psia, \bigcirc 26 psia, \square 34 psia, \square 40 psia, \diamond 55 psia, ∇ 70 psia, \triangle 82 psia, \triangleleft 95 psia. The solid line is a least-squares fit of the data.



3. A tracing of the time variation of the azimuthal magnetic field, its time derivative, and the laser pulse. Probe location is 4.0 mm before the orifice and 5.0 mm away from centerline. The target was nitrogen gas at a pressure of 40 psia. The laser had a peak power of 360 MW.



4. Variation of magnetic-field strength with the ratio of laser power to plenum pressure. The symbol shape denotes the plenum pressure: \triangleright 14 psia, \circ 26 psia, \square 34 psia, \diamond 40 psia, ∇ 55 psia, \odot 64 psia, \triangle 82 psia, \triangleleft 95 psia, ∇ 115 psia, \triangleright 160 psia, ∇ 210 psia. The symbols with vertical bars represent data obtained with the metallic housing. For this data the probe was 4.0 mm before the orifice and 5.0 mm away from centerline. The short-dash line through the data represents a least-squares fit. All remaining data shown were obtained with the nonconducting housing and with the probes located 1.8 mm before the orifice. The filled and half-filled symbols are for runs in which breakdown occurred 1.4 ± 0.2 mm before the orifice. The filled symbols and the solid line are for the probe located 5.5 mm from the centerline, whereas the half-filled symbols and the dash line are for the probe located 4.0 mm from the centerline. The open symbols and the long-dash line are for runs in which breakdown occurred 2.2 ± 0.2 mm before the orifice and the probe was located 5.5 mm from the centerline. The straight lines through the data obtained with the nonconducting housing were drawn with a slope of $1/3$.


UNCLASSIFIED
SECURITY CLASSIFICATION OF THIS PAGE (When Data Entered)

REPORT DOCUMENTATION PAGE		READ INSTRUCTIONS BEFORE COMPLETING FORM
1. REPORT NUMBER 18 AFOSR TR-77-0806	2. GOVT ACCESSION NO.	3. RECIPIENT'S CATALOG NUMBER
4. TITLE (and Subtitle) 9 TWO DIMENSIONAL EFFECTS IN LASER SOLID SIMULATION STUDIES	5. TYPE OF REPORT & PERIOD COVERED Scientific Final, 1 Aug. 1973 through 31 July 1976	
7. AUTHOR(s) 10 J. W./Daiber H. M./Thompson	6. PERFORMING ORG. REPORT NUMBER WG-5376-A-3	
9. PERFORMING ORGANIZATION NAME AND ADDRESS Calspan Corporation P. O. Box 235 Buffalo, New York 14221	8. CONTRACT OR GRANT NUMBER(s) 15 F44620-74-C-0004	
11. CONTROLLING OFFICE NAME AND ADDRESS Physics Division, Office of Scientific Research (AFSC), Bolling AFB, Bldg. 410 Washington, D. C. 20332	10. PROGRAM ELEMENT, PROJECT, TASK AREA & WORK UNIT NUMBERS 16 9767-04 17 61102F	
14. MONITORING AGENCY NAME & ADDRESS (if different from Controlling Office) 14 CALSPAN-WG-5376-A-3	12. REPORT DATE 11 October 1976	
16. DISTRIBUTION STATEMENT (of this Report) Approved for Public Release - Distribution Unlimited	13. NUMBER OF PAGES 12 35 P.	
17. DISTRIBUTION STATEMENT (of the abstract entered in Block 20, if different from Report)	15. SECURITY CLASS. (of this report) Unclassified	
18. SUPPLEMENTARY NOTES TECH, OTHER	15a. DECLASSIFICATION/DOWNGRADING SCHEDULE	
19. KEY WORDS (Continue on reverse side if necessary and identify by block number) Ruby Laser Free-jet Laser-Matter Interaction Plasma Laser Induced Waves Spontaneous Magnetic Fields		
20. ABSTRACT (Continue on reverse side if necessary and identify by block number) The objective of this program was to study the two-dimensional wave motions induced in a target by high-power laser radiation. For these studies the target is an axisymmetric, supersonic free-jet of gas which is laser irradiated on axis. The transparency of the target permits luminosity and schlieren streak photography of the waves that propagate into the high-pressure plenum. Measurements of the axial and lateral luminous-plasma growth and of the axial shock-wave growth in the plenum have been obtained over a range of plenum pressures		

UNCLASSIFIED

SECURITY CLASSIFICATION OF THIS PAGE(When Data Entered)

and laser powers. It has been found that the axial luminous-front growth can be predicted by a deflagration model; in this model the velocity scales with absorbed power divided by gas reservoir pressure to the one-third power. The temperature of the gas behind the deflagration wave is predicted to vary with the velocity squared. Temperature measurements which utilized metal-foil spectrometers to determine the relative x-ray flux in two wavelength intervals substantiated this scaling relation. The lateral expansion was found to be very slow, not even extending to the limits of the cone illuminated by the laser. Spontaneous magnetic fields are known to surround solid target during laser heating of their surfaces. Coil probes were used to determine if such fields existed near the laser-irradiated free-jet target and to measure the strength of these fields at several radial locations. An extrapolation of the data to the surface of the plasma indicate that azimuthal fields in excess of a megagauss exist. Such fields could retard the expansion of the plasma.



UNCLASSIFIED